FULL PAPER

Solution and/or mechano-mechanical synthesis of halogen and/or chalcogen bonded complexes: A crystal packing, solid state NMR and computational study

Shiv Kumar,[a] Carole Body,[b] Tom Leyssens, [b] Kristof Van Hecke, [c] Gilles Berger,[a] Arie Van der Lee,[d] Danielle Laurencin,[e] Sébastien Richeter,[e] Sébastien Clément, [e] and Franck Meyer*[a]

Dedication ((optional))

[a] Title(s), Initial(s), Surname(s) of Author(s) including Corresponding Author(s)
Department
Institution
Address 1
E-mail:
[b] Title(s), Initial(s), Surname(s) of Author(s)
Department
Institution
Address 2

Supporting information for this article is given via a link at the end of the document.((Please delete this text if not appropriate))

Abstract: Insert abstract text here. ((Abstracts should be 800-1000 characters in length excluding spaces. Please ensure your abstract is written so that it can be read in isolation (i.e., in an abstracting service such as PubMed), with all abbreviations defined.))

Introduction

The fabrication of next generation of nanoelectronic devices will require controlling the organization of components at the nanometer scale. To achieve this task, “top-down” or “bottom-up” strategies represent the two main techniques to create 2 or 3 dimensional highly ordered nanostructures.[1] Whereas the former may be deemed too costly to reach a degree of miniaturization lower than 10 nm by a lithographic approach, the latter can rely on the self-assembly of purpose-built elemental constituents through recognition processes in a highly reliable fashion. The bottom-up construction of nanoscale architectures can thus benefit of the wide array of non-covalent interactions of the supramolecular toolbox.[2]

Among the various molecular design principles of effective conducting materials, fluorine substitution stands for a very appealing strategy through lowering the HOMO level, and acting on morphological aspects by intra- or intermolecular S···F, H···F or π···F interactions.[3] On a parallel scene, halogen bonding (XB), i.e. the ability of a halogen to work as an electron density acceptor, has accounted for an upsurge of interest in the scientific community in the last two decades.[4][5] This interaction was initially reported as an intermolecular force in crystal engineering. In recent studies, some remarkable features like a high directionality, hydrophobicity or tunable strength allowed XB to be harnessed successfully in biological and materials sciences.[6][7] In the field of electronic materials, XB was already used to guide the arrangement of molecules, as observed in tetrathiafulvalene (TTF) chemistry.[8] In the same spirit, an improved 3D organization of poly(3-(ω-bromoalkyl)thiophenes) compared to poly(3-alkylthiophenes) was attributed to S···Br contacts.[9] From a physical point of view, XB was found to enhance the performance of perovskite and dye-sensitized solar cells through reduction of the recombination rate constant and regeneration of the dye, respectively, due to X···I^- interactions (X = Cl, Br, I).[10][11] Halogenation can thereby exert different levels of control over the performance of these functional materials.

Thiophene derivatives are versatile and key constituents of many conducting materials.[12] It has already been demonstrated that the supramolecular features of these building blocks can be translated at the macromolecular level to govern the organization of corresponding unit-containing polymers.[13] With this in mind, we decided to investigate the supramolecular organization of modified thiophenes by halogen bonding.[14] Several works have already reported the X-ray structures of halogen bonded arrays based on brominated compounds at positions 2 and/or 5, along with other bromine-containing analogs.[15] Herein, we turned our attention toward heterocycles functionalized at position 3 with pyridyl or tetrafluoroiodobenzene groups in combination with complementary XB donor or acceptor partners.[16] To shed light on the specificities of these molecular assemblies and to gather valuable information, thorough studies were conducted by single crystal X-ray diffraction. Interestingly, the halogen and chalcogen bonds team up in some complexes, sometimes unexpectedly. Density Functional Theory (DTF) investigations aimed at emphasizing the contribution of these interactions on the formation of these supramolecular architectures.[17][18] Finally, the preparation of polymorphic adducts was performed by solution and mechano-mechanical synthesis followed by a ^{13}C solid state NMR (SSNMR) spectroscopic analysis.

Results and Discussion

The formation of 3-((2,3,5,6-tetrafluoro-4-iodophenoxy)methyl)thiophene **ThioI** and 4-(thiophen-3-ylmethoxy)pyridine **ThioPy** as XB donor and acceptor, respectively, was carried out according to a procedure already described in the literature.[14] For the sake of comparison, 3-((perfluorophenoxy)methyl)thiophene **ThioF**, i.e. the analog of **ThioI** lacking the ability to make XB, was also prepared. For this, 3-thiophenemethanol has reacted with hexafluorobenzene in the presence of NaH, providing the corresponding **ThioF** in 98% yield (Figure 1).

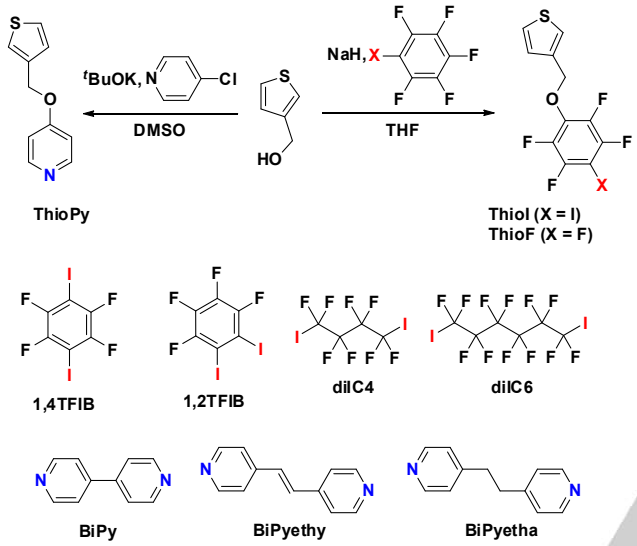

Figure 1 Syntheses of thiophene derivatives **ThioPy**, **ThioI** and **ThioF** (top). Halogen bond donors and acceptors used in that study (bottom).

X-ray structures of pure ThioI and ThioF

Subsequently, the crystallization of pure halogenated thiophenes **ThioI** and **ThioF** was performed through the slow evaporation of a dichloromethane solution of both compounds, giving rise to suitable materials for an X-ray diffraction analysis. The crystal packing of **ThioF** follows a columnar stacking arrangement in a head-to-tail fashion due to a π···π stacking between the aromatic groups that resembles that observed for (*E*)-3-(2,3,4,5,6-pentafluorostyryl)-thiophene (Figure 2 top).[19] The distance between the centroids of the electron rich thiophene ring and electron deficient pentafluoroarene varies in the range of 3.671-3.897 Å. The supramolecular architecture is also stabilized by several weak intermolecular H···F contacts (distances in the range of 2.539-2.620 Å) involving molecules in the same plane (H2···F8, H5···F10 and H5···F11) and π-stacked units (H6B···F12). In addition to these hydrogen bonds, halogen and chalcogen bonds contribute to the crystal cohesion through the connection of head-to-head orientated thiophenes belonging to neighboring column. Here, F10···F11 interactions arise as very weak XB (distance = 2.884 Å, i.e. around 98% of the sum of van der Waals radii).[20] The C-F10···F11 and C-F11···F10 angles are ~163.7° and ~134.2°, respectively, that could be consistent with halogen bonds of type II. Moreover, this structure is comprised of S···S contacts (distance = 3.673 Å) that falls within the limit of the sum of van der Waals radii (3.6 Å). It also exists a very short distance between sulfur and fluorine (3.323 Å) but the separation is slightly longer than the sum of van der Waals radii (S + F = 3.27 Å). It is worth mentioning that weak intermolecular interactions are characterized by stabilization energies up to 0.4 Å larger than the sum of van der Waals distance.[21]

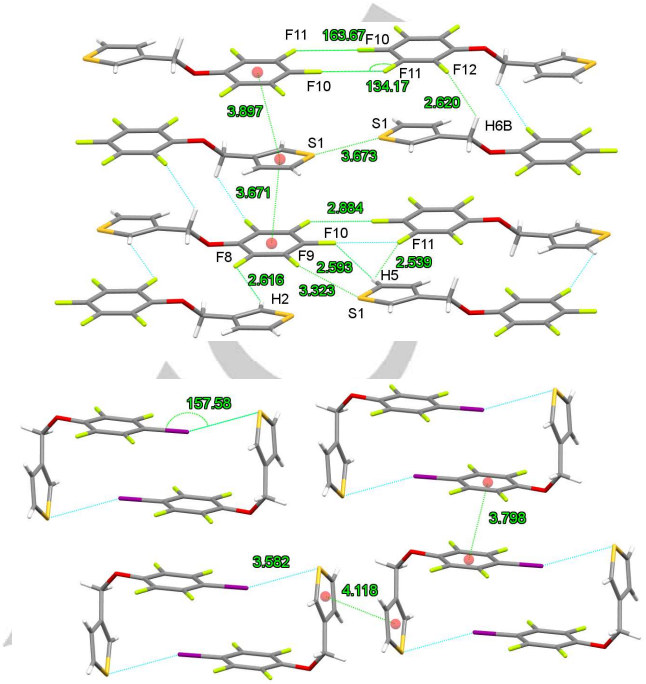

Figure 2. X-ray structure of **ThioF** organized in a head-to-tail fashion due to π···π stacking between the aromatic groups (top). X-ray structure of **ThioI** developing circular motifs due to S···I halogen bonds. The thiophene and perfluoroiodobenzene groups belong to planes (pale blue) making an angle of ~78° (bottom). The red dots represent the centroid of the aromatic rings. Colours are as follows: C, grey; H, white; F, yellow; S, orange; O, red; I, purple.

Replacement of fluorine by iodine on the fluorinated arene leads to a dramatic change of arrangement. **ThioI** units are now linked due to S···I halogen bonds (Figure 2 bottom). The S···I distance (3.582 Å) is around 6% shorter than the sum of van der Waals radii and the S···I-C angle is about 157° which is consistent with the electron-donation from sulfur to iodine. Although weak, this contact seems to govern the supramolecular arrangement that is composed of circular motifs of paired molecules. Each unit adopts an L-shape conformation in which the thiophene and tetrafluoroiodobenzene groups are almost perpendicular (~78°) (Figure S4). The overall architecture is also supported by π-stacked thiophene (centroid distance = 4.118 Å) and perfluoroarene (centroid distance = 3.798 Å) rings belonging to neighboring couples of molecules.

After the determination of the effective role of **ThioI** as halogen bond donor, the X-ray structure of **ThioPy** was then studied. Interestingly, two attempts of crystallization of **ThioPy** in dichloromethane and a mixture dichloromethane/hexane gave rise to two polymorphic forms called **ThioPya** and **ThioPyb**, respectively. In the first case, thiophene units of **ThioPya** develop a planar arrangement in a herringbone style due to H···O hydrogen bonds (2.518 Å) linking adjacent molecules (Figure 3 top). Moreover, the supramolecular architecture is stabilized by additional H···N and H···O hydrogen bonds with distances of 2.537 and 2.680 Å, respectively, involving molecules of parallel planes due to the twisted angle of ~89° made by the thiophene and pyridyl rings. Surprisingly, the X-ray structure of **ThioPyb**

obtained from the solvent mixture revealed a totally different pattern (Figure 3 bottom). A linear arrangement of units is obtained thanks to intermolecular S···N chalcogen bonds. The crystallographic data highlight a separation of 3.065 Å which represents 91.5% of the sum of van der Waals radii. Other weak hydrogen bonds operate between the parallel chains, namely H···O (2.854 Å) and H···π interactions (H···centroid distance = 3.430 Å).

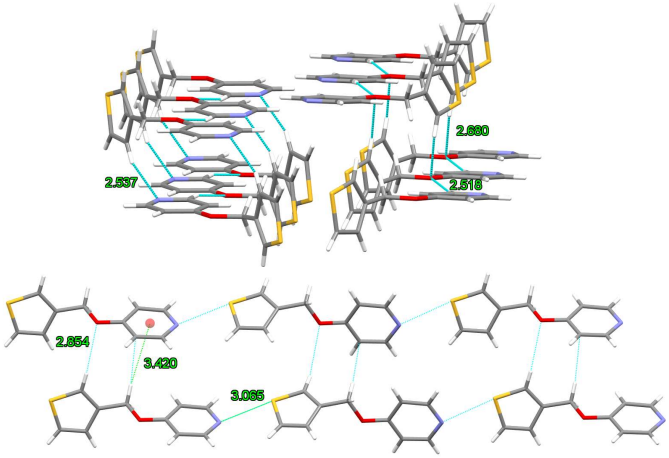

Figure 3. X-ray structures of polymorphic forms of **ThioPy** developing a herringbone pattern due to H···O hydrogen bonds in **ThioPya** (top) and a linear arrangement due to S···N chalcogen bonds in **ThioPyb** (bottom).

The X-ray structures of pure thiophenes **ThioI** and **ThioPy** confirmed the role of the aromatic groups as structure directing agents for these supramolecular assemblies. In a second step, we investigated the co-crystallization of these building blocks with selected partners.

X-ray structures of co-crystals involving ThioPy and diiodoperfluorinated compounds

Halogenoperfluorinated compounds are commonly used in halogen bonding driven self-assemblies. Indeed, the strong electron withdrawing fluorine atoms behave as activating agents towards the associated halogens through increasing their σ-hole size. Furthermore, the rod-like character of the perfluorinated core allows for a reliable transfer of molecular information.[22]

Firstly, **ThioPy** and diiodoperfluorobutane **diIC4** were co-crystallized, leading to a supramolecular trimeric structure due to N···I halogen bonds (Figure 4 top). These interactions appear much stronger than the previous S···I contacts found in **ThioI** since the distance between both atoms is 2.817 Å, i.e. about 20% shorter than the sum of van der Waals radii. Here, the N···I-C angle is almost linear (~170°). In this complex, we can consider that S and N compete to make XB with I, but the strongest prevails. These trimeric systems developed undulating chains making an angle of about 93° with thiophene rings at both extremities pointing toward another one, as observed in **ThioPya**. The stabilization of this architecture is also ensured by weak H···O hydrogen bonds (2.530 Å) that link parallel trimers.

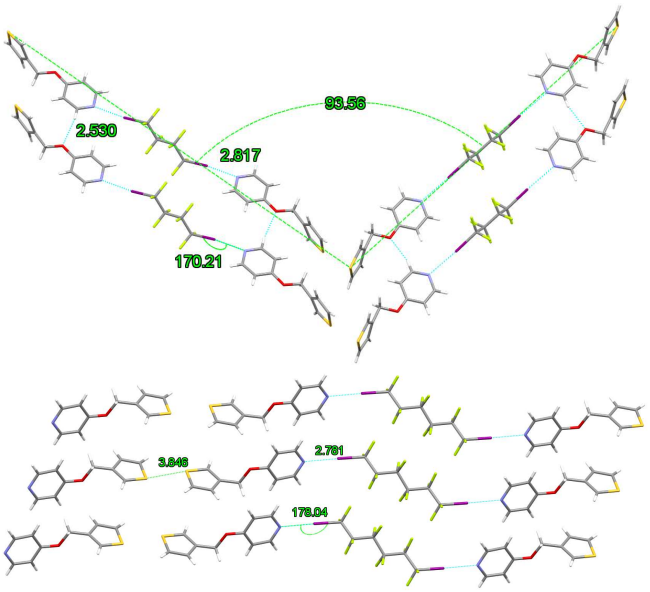

Figure 4. X-ray structures of halogen bonded complexes **ThioPy-diIC4** (top) and **ThioPy-DiIC6** (bottom)

Subsequently, we proceeded by the self-assembly of **ThioPy** with a longer analog, i.e. diiodoperfluorohexane (**DiIC6**) (Figure 4 bottom). In a similar way, the telechelic perfluorinated unit links both compounds into a trimeric structure due to N···I halogen bonds. These interactions appear slightly stronger than in the previous case, since the N···I separation drops to 78% of the sum of van der Waals radii, and the N···I-C angle makes ~178°. However, a comparison of **ThioPy-diIC4** and **ThioPy-diIC6** at the macromolecular level highlights a different organization. The repetition of the trimeric architecture forms infinite parallel chains with two thiophene rings pointing towards each other. The S···S separation is measured at 3.846 Å which is slightly longer than the sum of van der Waals radii. All units belonging to parallel planes run in the same direction which is in contrast with **ThioPy-diIC4** considering the zig-zag motif (Figure S5). Finally, the planar organization features a clear segregation between **ThioPy** and **DiIC6**, emphasizing the low affinity between perfluorocarbons and hydrocarbons. It is worthy of note that this aspect is also seen in **ThioPy-diIC4**.

Then, we turned our attention towards diiodoperfluoroarenes. In particular, 1,4-diiodotetrafluorobenzene (**1,4TFIB**) belongs to a class of halogen bond donors that has been frequently engaged in supramolecular functional materials.[23] Some relevant findings concern its role on the construction of organic cocrystal microlasers and haptic memory materials.[24][25] Interestingly, **ThioPy-1,4TFIB** and **ThioPy-diIC6** complexes develop a similar linear organization (Figure 5 top). The halogen bonded parameters appear almost identical (N···I distance = 2.757 Å, N···I-C angle ~178°) whereas a very short distance separates the thiophene groups. Now, the S···S contact is measured at 3.657 Å which is within the limit of the sum of van der Waals radii. From these results, it remains difficult to explain the structural variation from zig-zag (**ThioPy-diIC4**) to linear (**ThioPy-1,4TFIB** and **ThioPy-diIC6**) chain. A common feature of **ThioPy-1,4TFIB** and **ThioPy-diIC6** lies in almost identical geometrical parameters for XB. In **ThioPy-diIC4**, the slightly weaker halogen bonding strength could induce a change of orientation of **ThioPy** unit. The

absence of conjugation in **ThioPy** core prevents any competitive/cooperative phenomenon of electron transfer due to intermolecular interactions.[26] Further theoretical calculations will consider the S···S chalcogen bond strength.

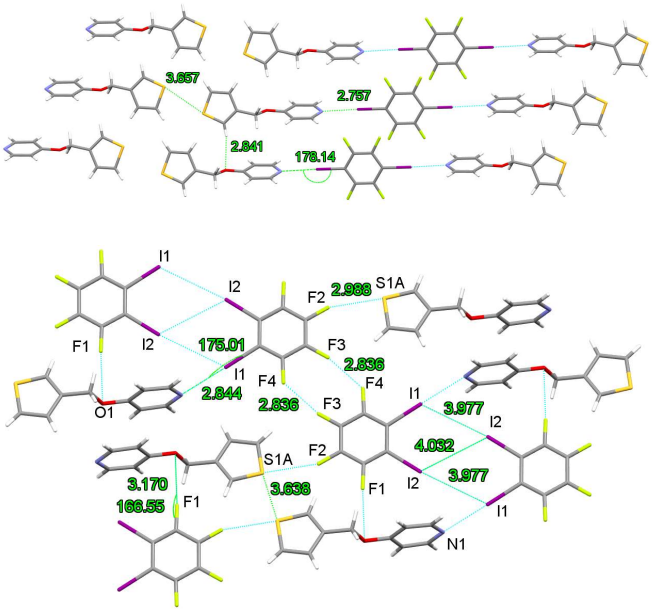

Figure 5. X-ray structures of halogen bonded complexes **ThioPy-1,4TFIB** (top) and **ThioPy-1,2TFIB** (bottom)

The use of 1,2-diiodotetrafluorobenzene **1,2TFIB** as halogen bonded building block is less reported compared to **1,4TFIB**, probably due to the difficulty to anticipate the geometry of the resulting complex. However, recent works have highlighted its potential in inducing phosphorescence in the presence of diazaphenanthrenes and on the ordering of photoresponsive block copolymers.[27][28] The co-crystal formation involving **ThioPy** and **1,2TFIB** led to a supramolecular architecture with an undefined pattern. In that case, a multitude of non-covalent bonds co-exist in which almost all halogen atoms of **1,2TFIB** are involved. As expected, **ThioPy** and **1,2TFIB** are linked through a strong N···I interaction, but only one iodine atom is involved which is a quite uncommon feature in light of the literature (Figure 5 bottom).[29] The crystallographic parameters show a N···I separation of 2.844 Å (~ 80% of the sum of van der Waals radii) and a N···I-C angle of 175°. In addition, short distances between iodine atoms arise within the limit of precision for halogen bonds of type I and II, taking into consideration the sum of van der Waals radii for iodine (3.96 Å). First, an electron donation from I1 towards I2 (XB of type I) can be concluded from the data since the I1···I2 distance is 3.977 Å whereas C-I1···I2 and C-I2···I1 angles are 119.2° and 173.9°, respectively. Moreover, a very weak contact consistent with a XB of type II is also present between I2 atoms, as revealed by a distance of 4.032 Å, associated with identical C-I2···I2 angles of 118.9°.[30] Moreover, the supramolecular arrangement is supported by weak F3···F4 halogen bonds (distance = 2.836 Å, i.e. around 96% of the sum of van der Waals radii). Values for C-F3···F4 and C-F4···F3 angles are different (155.9° and 135.5°, respectively) that could be in line with type II contacts. Surprisingly, F1 points towards the oxygen atom of **ThioPy**, but the distance (3.170 Å) appears slightly longer than the sum of van der Waals radii (O + F = 2.99 Å). It is worth noting that examples showing a fluorine atom as a halogen bond donor are scarce in the literature.[31] for instance, the first examples of $C_{sp3}F \cdots O_{sp3}$ interaction were reported in palladium complexes only in 2019.[32] Finally, S···S and S···F2 chalcogen bonds of 3.638 Å and 2.988 Å, respectively, lock the structure that give rise to a planar organization of these modules.

X-ray structures of co-crystals involving Thiol and bipyridyl derivatives

In a second step, we decided to reverse the code through the self-assembly of **Thiol** and bipyridyl derivatives, namely bipyridine ethane (**BiPyetha**), bipyridine ethylene (**BiPyethy**) and bipyridine (**BiPy**). As such, the self-assembly of **Thiol** with **BiPyetha** was operated in a mixture of dichloromethane/hexane using a 2:1ratio, respectively, considering the potential complementary functional groups for XB of both compounds. The X-ray structure analysis reveals a similar arrangement to the one found for **ThioPy-DiIC6** (Figure 6 top). Indeed, both modules form a trimeric system due to N···I halogen bonds, in which the interatomic distance is 2.791 Å (79% of the sum of van der Waals radii) with an almost linear N···I-C angle (~174°). In the same way, successive trimers develop a chain with thiophene rings pointing towards each other. The S···S separation is slightly shorter than in **ThioPy-DiIC6** (3.728 Å) but it remains longer than the sum of van der Waals radii for S. These thiophene groups are also hydrogen bonded with a neighboring **Thiol** unit due to two H···F contacts of 2.620 and 2.675 Å, respectively.

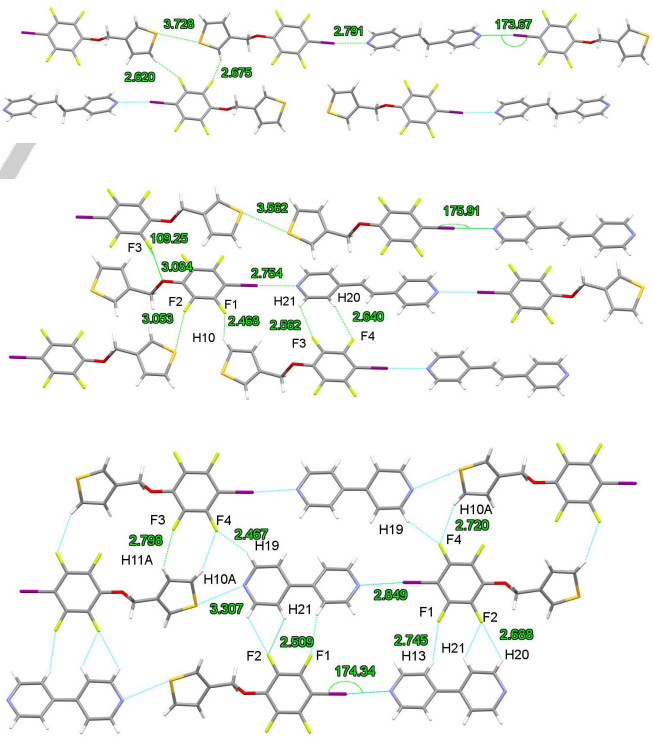

Figure 6. X-ray structure of halogen bonded complex **Thiol-BiPyetha** (top), **Thiol-BiPyethy** (middle) and **Thiol-BiPy** (bottom)

Following the same principle, **Thiol** and **BiPyethy** were co-crystallized under the same conditions. The supramolecular organization mirrored that observed for **Thiol-BiPyetha** (Figure 6 middle). N···I interactions held together three units, the crystallographic data being in agreement with a halogen bonding between N and I (N···I distance = 2.754 Å and N···I-C angle ~176°). In the same way, the linear arrangement of compounds reveals thiophene rings pointing toward each other, but in contrast to the previous case, the S···S distance is now lower than the sum of van der Waals radii (3.562 Å). This architecture is also comprised of other weak contacts linking parallel chains that give rise to planar systems. Hence, S···F2 chalcogen bonds of 3.053 Å (~7% interactions of the sum of van der Waals radii) are supplemented by three H···F hydrogen bonds of 2.468 Å (H10···F1), 2.562 Å (H21···F3) and 2.640 Å (H20···F4). As for complex **ThioPy-1,2TFIB**, two thiophenes belonging to parallel planes show a short O···F distance of only 3.084 Å (O···F4-C angle ~109°).

Finally, complex **Thiol-BiPy** highlighted the most surprising system (Figure 6 bottom). By comparison with the other **Thiol**-bipyridine family, both modules develop a linear arrangement, but N···I interactions are supplemented by N···S chalcogen bonds, leading to infinite chains running in opposite directions. XB seems slightly weaker than in the previous complexes (N···I distance = 2.849 Å and N···I-C angle ~174°) whereas the N···S distance (3.307 Å) represents a very weak interaction considering the sum of van der Waals radii (S+N = 3.35 Å). In that complex, parallel chains are also stabilized due to a plethora of H···F hydrogen bonds.

X-ray structure of complementary thiophenes Thiol-ThioPy obtained by solution synthesis

As aforementioned, the supramolecular organizations of two polymorphic structures of complementary thiophenes **Thiol-ThioPy** (called **Thiol-ThioPy A** and **Thiol-ThioPy B**, see Figures S6 and S7) were already studied in a previous work.[33] Crystals of **Thiol-ThioPy A** and **Thiol-ThioPy B** were grown from dichloromethane/hexane and acetone, respectively. Surprisingly, a third halogen bonded complex **Thiol-ThioPy C** has co-crystallized using XXX as solvent (Figure 7). From a general point of view, **Thiol-ThioPy B** and **Thiol-ThioPy C** are almost isomorphic. Only minor variations of crystallographic parameters are observed such as a shorted N···I distance (2.832 Å in **Thiol-ThioPy B** vs 2.794 Å in **Thiol-ThioPy C**) and H···F contacts in the latter compound. At the molecular level, both units adopt a very close conformation with an almost orthogonal orientation of pyridyl and thiophene groups in **ThioPy** unit (angle ~79°) whereas the aromatic rings of **Thiol** belong to nearly parallel planes (angle ~5°). The main difference appears between **Thiol-ThioPy A** and **Thiol-ThioPy C** since a superposition of couples of molecules occur in **Thiol-ThioPy A** whereas the halogen bonded pairs are slightly staggered in **Thiol-ThioPy B** and **Thiol-ThioPy C** (Figure 7 and S7).

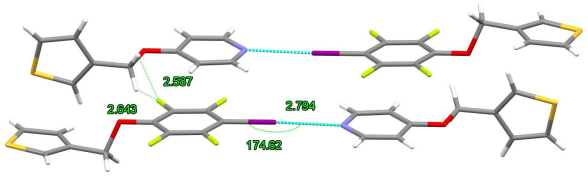

Figure 7. X-ray structure of halogen bonded complex **Thiol-ThioPy C**

Mechano-mechanical syntheses of Thiol-ThioPy complexes

Controlling and understanding the formation of different polymorphs is of crucial importance considering the associated structure-property relationship at the molecular or bulk level. To purposely address this issue, the mechano-mechanical synthesis of **Thiol-ThioPy** was carried out by ball milling in neat condition and through a liquid-assisted grinding (LAG) method using methanol, toluene, THF, water and dichloromethane (+/-0.25 μL/mg). Subsequently, the supramolecular materials were characterized by X-ray powder diffraction (XRPD) and compared to the starting compounds as well as **Thiol-ThioPy** complexes obtained by solution synthesis (see Figures S8-S15). Although XRPD spectra for **Thiol-ThioPy B** and **C** are almost identical, the peak at 2Θ = 24° found for **Thiol-ThioPy B** allowed to differentiate the two. It came out that **Thiol-ThioPy A** was obtained under neat and methanol-assisted grinding whereas **Thiol-ThioPy B** formation took place only by LAG using toluene, THF, water and dichloromethane (Table 1). The protic character and polarity of a solvent can have an influence on yielded forms. Here, no trend is observed considering that highly polar and protic methanol and water lead to different polymorphs.

Table 1. Preparation of **Thiol-ThioPy** complexes by ball milling in neat condition and LAG (+/- 0.25 μL/mg)

conditions	Dielectric constants[34][35]	isolated complexes
Neat	-	**Thiol-ThioPy A**
Methanol	32.6	**Thiol-ThioPy A**
Water	78.5	**Thiol-ThioPy B**
Toluene	2.41	**Thiol-ThioPy B**
Dichloromethane	8.9	**Thiol-ThioPy B**
THF	7.4	**Thiol-ThioPy B**

Both polymorphs were shown to be stable at room temperature for over a month (Figure SXXXX). Creating a supersaturated suspension in acetone containing both forms A and B, leads to a full transformation to form A, showing this latter to be the thermodynamically stable form at this temperature (Figure SXXXX). Both forms show close lying melting temperatures of 69°C, which lies between the melting points of Thiol (63°C) and of ThioPy (84°C) (Figures SXXX to SXXXX).

^{13}C solid state NMR spectroscopy analysis

SSNMR has become an important analytical tool which complements X-ray crystallography, particularly for disordered systems and structures showing internal dynamics.[36] As far as the study of halogen bonded complexes is concerned, only an handful of instances has emphasized chemical shift variation relative to pure compounds by ^{15}N, ^{13}C, ^{31}P, ^{17}O or ^{35}Cl SSNMR.[37] Considering the potential need to highlight XB in modified thiophenes-based macromolecular materials, ^{13}C SSNMR analyses were carried out for solid samples **Thiol**, **ThioPy** and **Thiol-ThioPy**. The ^{13}C SSNMR spectrum of **Thiol-ThioPy** reveals a shift to higher frequencies of the C-I resonance

(C9) compared to pure **Thiol**, consistent with results reported elsewhere (Figure 8~~Figure 8~~).[38] Variation of chemical shifts for C8, C8' and C7, C7' relevant?

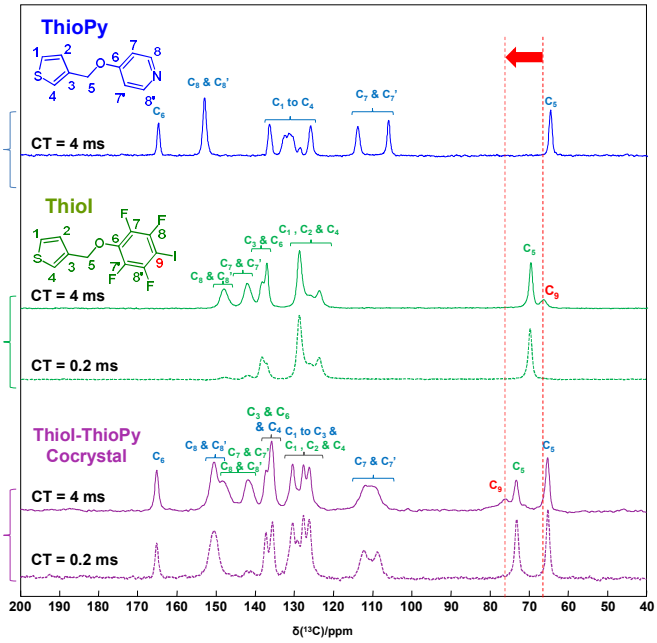

Figure 8. ^{13}C solid state NMR spectra of **ThioPy** (blue), **Thiol** (green) and the **Thiol-ThioPy** cocrystal (purple), showing the shift in the C-I resonance (C9) upon formation of the halogen bonded co-crystal.

N···S chalcogen bonds in the Cambridge Structural Database

In the last few years, chalcogen bonds have gain increasing attention in chemical sciences and protein-ligand complexes due to similarities with the halogen bonds, namely an anisotropic charge distribution.[39][40] Typically, the ability of an element of group 16 to form chalcogen bonds is dependent of neighboring residues. Hence, electron withdrawing groups tend to increase the size of the positive σ hole of the chalcogen atom that gives rise to stronger attractive interactions. Moreover, selenium and tellurium are more polarizable chalcogen atoms than S that make the latter less prone to recognition processes.[41] Whereas intramolecular N···S interactions are frequently encountered in stabilizing a planar conformation (e.g. in conducting materials),[42] the same contacts are less reported at the intermolecular level. In order to address the unusual N···S chalcogen bond observed in **Thiol-BiPy**, a preliminary Cambridge Structural Database (CSD) survey (version 2021.1, 5.42 updates May 2021) was carried out focusing on structures comprised of S and N atoms connected to 2 C atoms with N···S distance lower than 3.35 Å. It came out 181 compounds involved in inter- or intramolecular interactions. This amount drops to 13 structures considering thiophene and pyridine derivatives, all of these being homo-crystals (see supporting information). A step further, we focus on crystalline systems where two different units are linked through intermolecular N···S interactions. Only 5 molecular entities feature the same parameters (N···S distance < 3.35 Å), namely OGUTIV, NAQPUT, FAFSEL, SUKPAS and NUSLOE. In the charge transfer complex NUSLOE, the X-ray analysis reveals a π···π stacking between the aromatic groups of TTF and dicyanolumazine, leading to an N···S-C angle of ~80°.[43] In general, when S behaves as a nucleophile in such aromatic systems, electrophiles approach in a direction from 50 to 90° from the C-S-C plane, as seen in **Thiol**. So this instance should be out of consideration for an electron donation from N to S.[44] Finally, OGUTIV is also composed of bipyridine as electron donor toward the antibiotic sulfamethizole in the remaining complexes.[45] Therefore, N···S chalcogen bonds driven self-assemblies of complementary partners arise as a very rare phenomenon in crystal engineering.

Table 1. Table Caption. ((**Note:** Please do **not** include the table in a textbox or frame))

Head 1[a]	Head 2	Head 3[b]	Head 4[c]	Head 5
Column 1	Column 2	Column 3	Column 4	Column 5
Column 1	Column 2	Column 3	Column 4	Column 5

[a] Table Footnote. [b] …

Conclusion

Main Text Paragraph.

Experimental Section

Experimental Details.

Acknowledgements ((optional))

Acknowledgements Text.

Keywords: keyword 1 • keyword 2 • keyword 3 • keyword 4 • keyword 5

[1] B. Han, Z. Li, C. Li, I. Pobelov, G. Su, R. Aguilar-Sanchez, T. Wandlowski, *Top. Curr. Chem.* **2009**, *287*, 181–255.
[2] W. Lu, C. M. Lieber, *Nat. Mater.* **2007**, *6*, 841–850.
[3] F. Meyer, *Prog. Polym. Sci.* **2015**, *47*, 70–91.
[4] G. Cavallo, P. Metrangolo, R. Milani, T. Pilati, A. Priimagi, G. Resnati, G. Terraneo, *Chem. Rev.* **2016**, *116*, 2478–2601.
[5] L. C. Gilday, S. W. Robinson, T. A. Barendt, M. J. Langton, B. R. Mullaney, P. D. Beer, *Chem. Rev.* **2015**, *115*, 7118–7195.
[6] G. Berger, J. Soubhye, F. Meyer, *Polym. Chem.* **2015**, *6*, 3559–3580.
[7] G. Berger, P. Frangville, F. Meyer, *Chem. Commun.* **2020**, *56*, 4970–4981.
[8] M. Fourmigué, P. Batail, *Chem. Rev.* **2004**, *104*, 5379–418.
[9] A. Bocheux, I. Tahar-Djebbar, C. Fiorini-Debuisschert, L. Douillard,

F. Mathevet, A.-J. Attias, F. Charra, *Langmuir* **2011**, *27*, 10251–10255.

[10] A. Abate, M. Saliba, D. J. Hollman, S. D. Stranks, K. Wojciechowski, R. Avolio, G. Grancini, A. Petrozza, H. J. Snaith, *Nano Lett.* **2014**, *14*, 3247−3254.

[11] S. J. C. Simon, F. G. L. Parlane, W. B. Swords, C. W. Kellett, C. Du, B. Lam, R. K. Dean, K. Hu, G. J. Meyer, C. P. Berlinguette, *J. Am. Chem. Soc.* **2016**, *138*, 10406−10409.

[12] G. Barbarella, M. Melucci, G. Sotgiu, *Adv. Mater.* **2005**, *17*, 1581–1593.

[13] S. Clément, F. Meyer, J. De Winter, O. Coulembier, C. M. L. Vande Velde, M. Zeller, P. Gerbaux, J.-Y. Balandier, S. Sergeyev, R. Lazzaroni, Y. Geerts, P. Dubois, *J. Org. Chem.* **2010**, *75*, 1561–1568.

[14] G. Berger, J. Soubhye, A. Van Der Lee, C. Vande Velde, R. Wintjens, P. Dubois, S. Clément, F. Meyer, *Chempluschem* **2014**, *79*, 552–558.

[15] A.-L. Barrès, M. Allain, P. Frère, P. Batail, *Isr. J. Chem.* **2014**, *54*, 689–698.

[16] M. Baldrighi, P. Metrangolo, F. Meyer, T. Pilati, D. Proserpio, G. Resnati, G. Terraneo, *J. Fluor. Chem.* **2010**, *131*, 1218–1224.

[17] C. M. Widdifield, G. Cavallo, G. A. Facey, T. Pilati, J. Lin, P. Metrangolo, G. Resnati, D. L. Bryce, *Chem. - A Eur. J.* **2013**, *19*, 11949–11962.

[18] D. L. Bryce, J. Viger-Gravel, *Top. Curr. Chem.* **2008**, *358*, 183–203.

[19] S. Clément, O. Coulembier, F. Meyer, M. Zeller, C. M. L. Vande Velde, *Acta Crystallogr. Sect. E Struct. Reports Online* **2010**, *E66*, o896–o897.

[20] S. S. Batsanov, *Inorg. Chem.* **2001**, *37*, 1031–1046.

[21] I. Dance, *New J. Chem.* **2003**, *27*, 22–27.

[22] V. Kumar, T. Pilati, G. Terraneo, F. Meyer, P. Metrangolo, G. Resnati, *Chem. Sci.* **2017**, *8*, 1801–1810.

[23] X. Ding, Y. Chang, C. Ou, J. Lin, L. Xie, *Natl. Sci. Rev.* **2020**, *7*, 1906–1932.

[24] M. Chu, B. Qiu, W. Zhang, Z. Zhou, X. Yang, Y. Yan, J. Yao, Y. J. Li, Y. S. Zhao, *ACS Appl. Mater. Interfaces* **2018**, *10*, 42740–42746.

[25] L. Bai, P. Bose, Q. Gao, Y. Li, R. Ganguly, Y. Zhao, *J. Am. Chem. Soc.* **2017**, *139*, 436–441.

[26] G. Berger, K. Robeyns, J. Soubhye, R. Wintjens, F. Meyer, *CrystEngComm* **2016**, *18*, 683–690.

[27] Y. J. Gao, C. Li, R. Liu, W. J. Jin, *Spectrochim. Acta, Part A Mol. Biomol. Spectrosc.* **2017**, *173*, 792–799.

[28] Y. Chen, S. Huang, T. Wang, H. Yu, *Macromolecules* **2020**, *53*, 1486–1493.

[29] M. Du, L. Li, J. Zhang, K. Li, M. Cao, L. Mo, G. Hu, Y. Chen, H. Yu, H. Yang, *Liq. Cryst.* **2019**, *46*, 37–44.

[30] Q. J. Shen, H. Q. Wei, W. S. Zou, H. L. Sun, W. J. Jin, *CrystEngComm* **2012**, *14*, 1010–1015.

[31] K. Eskandari, M. Lesani, *Chem. - A Eur. J.* **2015**, *21*, 4739–4746.

[32] V. Elakkat, C.-C. Chang, J.-Y. Chen, Y.-C. Fang, C.-R. Shen, L.-K. Liu, N. Lu, *Chem. Commun.* **2019**, *55*, 14225–14392.

[33] G. Berger, J. Soubhye, A. van der Lee, C. Vande Velde, R. Wintjens, P. Dubois, S. Clément, F. Meyer, *Chempluschem* **2014**, *79*, 552–558.

[34] U. Mayer, V. Gutmann, W. Gerger, *Monatshefte für Chemie* **1975**, *106*, 1235–1257.

[35] B. R. Hyun, A. C. Bartnik, J. K. Lee, H. Imoto, L. Sun, J. J. Choi, Y. Chujo, T. Hanrath, C. K. Ober, F. W. Wise, *Nano Lett.* **2010**, *10*, 318–323.

[36] Y. Xu, P. M. J. Szell, V. Kumar, D. L. Bryce, *Coord. Chem. Rev.* **2020**, *411*, 213237.

[37] P. C. Vioglio, M. R. Chierotti, R. Gobetto, *CrystEngComm* **2016**, *18*, 9173–9184.

[38] J. Viger-Gravel, S. Leclerc, I. Korobkov, D. L. Bryce, *CrystEngComm* **2013**, *15*, 3168–3177.

[39] P. Scilabra, G. Terraneo, G. Resnati, *Acc. Chem. Res.* **2019**, *52*, 1313–1324.

[40] M. R. Koebel, A. Cooper, G. Schmadeke, S. Jeon, M. Narayan, S. Sirimulla, *J. Chem. Inf. Model.* **2016**, *56*, 2298–2309.

[41] J. Y. C. Lim, P. D. Beer, *Chem* **2018**, *4*, 731–783.

[42] C. Réthoré, A. Madalan, M. Fourmigué, E. Canadell, B. Elsa, M. Almeida, R. Clérac, N. Avarvari, *New J. Chem.* **2007**, *31*, 1468–1483.

[43] K. Sakai, K. Nagahara, Y. Yoshii, N. Hoshino, T. Akutagawa, *J. Phys. Chem. A* **2013**, *117*, 3614−3624.

[44] J. P. Glusker, in *Top. Curr. Chem. 198* (Ed.: E. Weber), Springer-Verlag Berlin Heidelberg, **1998**, pp. 1–56.

[45] K. Suresh, V. S. Minkov, K. K. Namila, E. Derevyannikova, E. Losev, A. Nangia, Elena V. Boldyreva, *Cryst. Growth Des.* **2015**, *15*, 3498−3510.

Entry for the Table of Contents

Insert graphic for Table of Contents here. ((Please ensure your graphic is in **one** of following formats))

((max. width: 5.5 cm; max. height: 5.0 cm))

Please delete this box prior to submission

((max. width: 11.5 cm; max. height: 2.5 cm))

Please delete this box prior to submission

Insert text for Table of Contents here. ((The Table of Contents text should give readers a short preview of the main theme of the research and results included in the paper to attract their attention into reading the paper in full. The Table of Contents text **should be different from the abstract** and should be no more than 450 characters including spaces.))

Institute and/or researcher Twitter usernames: ((optional))